PCCP

ROYAL SOCIETY OF CHEMISTRY

PAPER

View Article Online
View Journal

Check for updates

Cite this: DOI: 10.1039/d5cp04813c

Why is the eclipsed form of dimethylacetylene more stable than its staggered form?†

Volker Staemmler[a] and Robert Franke *[ab]

In organic molecules that exhibit conformational isomers—namely, a staggered and an eclipsed arrangement, as observed in compounds such as ethane or propane—the staggered conformation generally represents the equilibrium structure. This preference is commonly attributed to steric hindrance, Pauli repulsion or hyperconjugation. Surprisingly, in 2-butyne or dimethylacetylene the eclipsed form is lower in energy, but only by 0.017 kcal mol^{-1} or 5.98 cm^{-1}. The present study shows that in this case neither 'Pauli repulsion' nor 'hyperconjugation' plays the decisive role, but the kinetic energy of the electrons. A rigid rotation around the linear C–C≡C–C axis from the eclipsed equilibrium structure to the staggered one increases the electronic kinetic energy by as much as 0.126 kcal mol^{-1}, while the increase of the total energy is rather small. The rotationally symmetric ring of the π-orbitals around the acetylenic C≡C bond is modulated at three angles in the eclipsed conformer, but at six angles in the staggered one, and this causes the larger electronic kinetic energy. Of course, an increase of both the total energy and the electronic kinetic energy violates the virial theorem. This is then restored by a small increase of only 0.0008 Å in the C–C bond distances, which leads to an elongation and smoothing of the σ-orbitals at the C–C≡C–C axis and to a reduction of their kinetic energy. In addition to the explanation, why the energy of the eclipsed form of 2-butyne is lower than that of the staggered form, our calculations confirm the experimental observation that the rotation barrier in 2-butyne is very small, only about 6 cm^{-1}.

Received 11th December 2025,
Accepted 8th April 2026

DOI: 10.1039/d5cp04813c

rsc.li/pccp

Open Access Article. Published on 22 June 2026. Downloaded on 6/23/2026 3:22:00 AM.
This article is licensed under a Creative Commons Attribution 3.0 Unported Licence.

Introduction

The molecule 2-butyne or dimethylacetylene is not of importance in industrial or organic chemistry nor in biochemistry. The synthesis and essential physicochemical properties were first described in the 1930s.[1,2] It has attracted some interest during the last twenty years, mainly because of its rich spectroscopic properties. Starting from the unpublished PhD dissertation of H. Kaiser,[3] several groups have studied its UV spectrum experimentally, in particular the photoabsorption,[4–7] photoionization[8] and Rydberg spectra,[9] but also several IR bands.[10,11] A limited number of quantum chemical *ab initio* computations have been conducted, mainly to determine the geometrical structures of its distinct conformers.[5,12]

2-Butyne is structurally interesting in that it is the simplest alkyne that exhibits rotational isomerism, which therefore contains rotamers. According to IUPAC, rotamers are defined as: "One of a set of conformers arising from restricted rotation about one single bond".[13] Conceptually, this compound can be obtained from ethane by inserting a –C≡C– moiety between adjacent methyl groups. According to a term introduced by Houk *et al.* for pericyclines,[14] 2-butyne can also be referred to as "exploded ethane". Another designation that emphasizes the connection to ethane and goes back to Maraval and Chauvin[15] is to refer to 2-butyne as the *carbo*-mer of ethane. For more information on the topic of rotational isomerism in compounds containing acetylene groups, one is advised to refer to the comprehensive review article by Toyota.[16]

The electronic ground state of 2-butyne has a linear C–C≡C–C structure, as determined experimentally by crystallography[17] and electron diffraction.[18] Similar to ethane, the two terminal methyl groups can adopt either an eclipsed or a staggered orientation. However, in the earlier literature it was neither definitively known which one of the two possibilities is the equilibrium structure of the ground state, nor how large the rotational barrier might be.[16] In 1997, di Lauro *et al.*[11] determined it to be 5.98 ± 0.03 cm^{-1} (or 0.0171 kcal mol^{-1}), by analyzing the rotation-torsion structure of certain vibrational bands, but they could not decide which of the two structures is the true equilibrium geometry of the ground state.

All recent quantum chemical calculations, on the other hand, could establish that the ground state of 2-butyne has

[a] Lehrstuhl für Theoretische Chemie, Ruhr-Universität Bochum, D-44780 Bochum, Germany. E-mail: robert.franke@ruhr-uni-bochum.de
[b] Evonik Oxeno GmbH, Paul-Baumann-Str. 1, D-45772 Marl, Germany

† We dedicate this work to the late Martin Jungen, Professor for Theoretical Chemistry at the Universität Basel, Switzerland.

Open Access Article. Published on 22 June 2026. Downloaded on 6/23/2026 3:22:00 AM.
This article is licensed under a Creative Commons Attribution 3.0 Unported Licence.

an eclipsed structure, and they were able to get rather reliable values for the rotational barrier, despite of the fact that it is so very small. Palmer and Walker[5] obtained a value of 4.59 cm^{-1} by means of UHF-MP2 calculations with a TZVP basis set, Hong Xu *et al.*[8] reported a theoretical value of about 5 cm^{-1}, without mentioning the details of their calculations, and Omorodion *et al.*[12] obtained a value of 0.010 kcal mol^{-1} (or 3.57 cm^{-1}) at the CCSD(T) level for 2-butyne itself and similar, but slightly larger, values for several substituted 2-butynes.

Present calculations

For our own calculations we started from geometries optimized at the Hartree–Fock (HF) level and with density functional theory (DFT) employing the B3LYP functional, both for the eclipsed and staggered forms of 2-butyne, in their D_{3h} and D_{3d} symmetries. The TURBOMOLE program package[19] and the def2-QZVPP basis set of Weigend *et al.*[20] were used for this purpose. The results are given in Table 1 and show that the C≡C and C-H distances as well as the CCH bond angles are nearly the same in the eclipsed and staggered geometry, while the C–C distance is slightly longer in the staggered form, but only by the tiny amount of 0.00008 Å. To further substantiate this result and, as far as possible, to assess whether contributions from electron correlation may influence the structural parameters, we additionally report geometry optimisations with the CCSD(T)-F12 code[21] of the TURBOMOLE package.[19] Table 1 shows that the bond lengths and angles obtained at the HF and B3LYP levels are very close to those obtained by CCSDT(T)-F12, except for C≡C bond length which is by 0.02 Å too short at the HF level. What is more important for our analysis is that the elongation of the C–C bond length from the eclipsed to the staggered form is nearly the same for all three geometry optimizations: 0.000076 Å, 0.000087 Å and 0.000072 Å at HF, B3LYP and CCSD(T)-F12. This indicates in particular that dynamic correlation effects do not play a significant role in this case.

The calculations for the total energies and for the analysis of their components were performed with our own HF[23,24] program and also with codes that contain correlation effects: with our own MCCEPA[25] program as well as with the CC2[26] and the CCSD(T)-F12[21] codes. (Of course, our multireference-CEPA program can also be applied to single reference electronic states.) With the three packages including correlation effects, CEPA, CC2 and CCSD(T), we got nearly the same results for the rotational barrier as with HF, therefore we used for analyzing the origin of the rotational barrier only the HF method.[23,24]

Table 1 Optimized geometries for 2-butyne (in Å and degrees); def2-QZVPP basis set[20] for the HF and DFT calculations, def2-TZVPP basis set[22] for CCSD(T)-F12

Method		Eclipsed (D_{3h})	Staggered (D_{3d})
HF	R(C≡C)	1.181742	1.181744
	R(C–C)	1.465507	1.465583
	R(C–H)	1.081702	1.081691
	<(CCH)	110.652	110.654
B3LYP	R(C≡C)	1.200476	1.200478
	R(C–C)	1.456718	1.456805
	R(C–H)	1.091216	1.091200
	<(CCH)	111.184	111.185
CCSD(T)-F12	R(C≡C)	1.207854	1.207856
	R(C–C)	1.463930	1.464002
	R(C–H)	1.089976	1.089965
	<(CCH)	110.766	110.766

Table 2 shows that our results for the rotational barrier of 2-butyne are very close to the experimental value of 5.98 cm^{-1},[11] at the HF, CEPA, CC2 and CCSD(T)-F12 levels, and also whether HF, B3LYP, CC2 or CCSD(T)-F12 optimized geometries had been used. Table 2 indicates that a TZP basis set is too small to reproduce such a tiny energy difference. And as it will be shown later, the rather large and popular def2-QZVPP basis set[20] yields a reliable value for the rotational barrier itself, but it is not flexible enough for our analysis. Therefore we used also the full ANO basis set of Widmark *et al.*[28] (including three f-sets at the C atoms) and a completely decontracted basis set, based on the basis of Huzinaga[29a] for H and on the well-tempered basis of Huzinaga and Klobukowski[29b] for C, extended by two steep s- and p- functions at the C atoms. This basis set will be denoted by HUZ-ext and is contained in the SI.

Pauli repulsion or hyperconjugation?

And now the question: What is the reason that in 2-butyne the eclipsed form is more stable than the staggered one, contrary to the situation in ethane? The case of ethane has been discussed in the literature many times. We recall only the two most popular, but completely different, explanations—"steric repulsion"[30] or Pauli repulsion and "hyperconjugation"[31]—and refer to our own paper[32] containing a more detailed discussion of this subject.

The rotational barrier in ethane is commonly attributed to Pauli repulsion: the electrons in the C–H bonds of adjacent CH_3 groups repel each other due to the Pauli principle. This repulsion is stronger in the eclipsed conformation than in the staggered one, because the bonds approach each other more closely in the eclipsed form.[30] A similar effect might be considered for 2-butyne. However, the distances between the C–H bonds of the terminal CH_3 groups are so large that any significant Pauli repulsion essentially disappears. Consequently, Pauli repulsion cannot account for the rotational barrier in 2-butyne.

A much more convincing idea is that hyperconjugation[31] might be the origin of the rotational barrier in 2-butyne. There are three pairs of molecular orbitals belonging to e-type irreducible representations (irreps) of the D_{3h} and D_{3d} molecules: The e-type combinations of the three CH bonding orbitals at the terminal CH_3 groups and the bonding π orbitals at the central C≡C bond. They can form three (doubly degenerate) delocalized e-type (or π-type) orbitals along the four-center C–C≡C–C chain. This is a typical case of hyperconjugation, where the π bond at the central C≡C triple bond extends a little over the neighbouring C–C single bonds. Of course, one would expect that the four-center bonding e-type orbital is lower in energy if the terminal CH_3 groups are "in phase", *i.e.* in the eclipsed form.

This journal is © the Owner Societies 2026

Open Access Article. Published on 22 June 2026. Downloaded on 6/23/2026 3:22:00 AM.
This article is licensed under a Creative Commons Attribution 3.0 Unported Licence.

Table 2 Calculated rotation barriers in 2-butyne (in E_h and cm^{-1})

Method[a]	Geometry[b]	Basis set	Energy (E_h) (eclipsed FR)	ΔE (E_h) (staggered FR)	ΔE (cm^{-1})
HF	HF	TZP	−154.95158804	+0.00001626	+3.57
HF	HF	def2-QZVPP	−154.97804570	+0.00002672	+5.86
HF	HF	ANO	−154.97801428	+0.00002702	+5.93
HF	HF	HUZ-ext[c]	−154.97871729	+0.00002771	+6.08
HF	B3LYP	def2-QZVPP	−154.97680920	+0.00002617	+5.74
B3LYP	B3LYP	def2-QZVPP	−155.94632967	+0.00002947	+6.47
CEPA	HF	def2-QZVPP	−155.67768677	+0.00002673	+5.86
CEPA	B3LYP	def2-QZVPP	−155.67830367	+0.00002381	+5.23
CC2	CC2	aug-cc-pV6Z[d]	−155.86418802	+0.00002498	+5.48
CCSD(T)-F12	HF	def2-TZVPP	−155.74247286	+0.00002078	+4.56
CCSD(T)-F12	B3LYP	def2-TZVPP	−155.73973460	+0.00002235	+4.91
CCSD(T)-F12	CCSD(T)-F12	def2-TZVPP	−155.74158429	+0.00002089	+4.58
Exp.[11]					+5.98 ± 0.03

[a] The excitations of the 1s orbitals on the four C atoms were not included in the treatments containing correlation effects (CEPA, CC2, CCSD(T)-F12). [b] Fully optimized geometries (FR), as shown in Table 1, both for the eclipsed and staggered form. [c] Completely decontracted and extended Huzinaga basis set. See Supporting Information. [d] See ref. 27.

Applying simple Hückel theory[33,34]—as Mulliken did as early as in 1941 to establish the concept of hyperconjugation[35,36]—provides an initial estimate of the energies of these three (doubly degenerate) orbitals. The Hückel matrix H and the corresponding energies of the three resulting Hückel-type orbitals are given in eqn (1)–(3). The energies ε_1 and ε_3 belong to the bonding and the antibonding orbital, ε_2 to the nonbonding one.

$$H = \begin{pmatrix} \alpha-\varepsilon & \gamma & 0 \\ \gamma & \beta-\varepsilon & \gamma \\ 0 & \gamma & \alpha-\varepsilon \end{pmatrix} \quad (1)$$

$$\varepsilon_2 = \alpha \quad (2)$$

$$\varepsilon_1 = \varepsilon_3 = \frac{\alpha+\beta}{2} \pm \sqrt{\left(\frac{\alpha-\beta}{2}\right)^2 + 2\gamma^2} \quad (3)$$

In Table 3 the orbital energies of 2-butyne in its optimized (in the following characterized by FR, fully relaxed) eclipsed and staggered forms are given, together with those of a third form (staggered RR), obtained from the eclipsed form with a rigid rotation (RR) around the C–C≡C–C axis. (The HF optimized geometries and the def2-QZVPP basis were used and the four C 1s orbital energies are omitted, because their changes are quite small.) The table indicates that the energies of the three-center bonding pair, ε_{10} and ε_{11}, are approximately 0.000050 E_h (E_h: Hartree, the atomic unit of energy, 1 E_h = 627.509 kcal mol^{-1}) lower in the eclipsed conformation compared to the two staggered conformations. Although this difference is small, the changes in the other two orbital energies are even smaller, in the order of ±0.000020 E_h. Thus, it can be concluded that hyperconjugation favors the eclipsed over the staggered form of 2-butyne.

However, in this simple Hückel approach the orbital energies ε_1, ε_2, ε_3 of eqn (2) and (3) are the same for the eclipsed and staggered forms of 2-butyne, therefore it cannot explain why the eclipsed form has a lower energy than one of the staggered forms. The reason is that in the Hückel matrix of eqn (1) only the coupling between the terminal CH_3 groups and the central C≡C π orbitals are included explicitly, by means of the off-diagonal matrix element γ. To determine the energy difference between the eclipsed and staggered conformations, one would have to introduce a nonzero value, *e.g.*, δ for the off-diagonal matrix element between the terminal CH_3 groups. However, this modification goes beyond the scope of the simple Hückel approach and, more critically, the resulting new energies ε_1, ε_2, ε_3 would include a term linear in δ, which may be positive or negative. Consequently, this does not allow us to conclude whether the eclipsed or the staggered conformer is more stable.

Table 3 Orbital energies (in E_h) of the orbitals 5 to 15 for the three forms of 2-butyne. HUZ-ext basis set

Orbital Nr. Structure[b]	Irrep[a]	Eclipsed FR	Staggered RR	Staggered FR
5	a	−1.063389	−1.063369	−1.063354
6	a	−1.001244	−1.001229	−1.001215
7	a	−0.920712	−0.920692	−0.920699
8	a	−0.648845	−0.648831	−0.648826
9	a	−0.594468	−0.594448	−0.594437
10, 11	e	−0.593056	−0.593011	−0.593005
12, 13	e	−0.576076	−0.576091	−0.576090
14, 15	e	−0.367382	−0.367360	−0.367368

[a] Only the a- or e- part of the irreps is indicated, because the further specification differs in the D_{3h} and D_{3d} symmetries. [b] FR = fully relaxed; HF optimized geometry; RR = rigid rotation, out of the HF-FR eclipsed geometry.

Although the proposition ''hyperconjugation is the origin of the rotational barrier in 2-butyne'' still appears quite convincing, two additional questions remain—beyond determining which of the two conformations is more stable:

(1) It is well known that in HF theory - and at more sophisticated levels as well - the sum of the orbital energies is not identical with the total energy.[37] Therefore, is it really allowed to conclude from one lower orbital energy to a lower total energy?

(2) Our optimized geometries, contained in Table 1, show that the C≡C and C–H bond lengths are nearly identical in the

Open Access Article. Published on 22 June 2026. Downloaded on 6/23/2026 3:22:00 AM.
This article is licensed under a Creative Commons Attribution 3.0 Unported Licence.

Table 4 Energy components (in E_h) for the different forms of 2-butyne; HF optimized geometry

Energies	Basis set	Eclipsed FR	Staggered RR	Staggered FR
E_{SCF}	def2-QZVPP	−154.97804570	−154.97801897	−154.97801898
T_{el}	def2-QZVPP	154.96409543	154.96428915	154.96406030
V	def2-QZVPP	−309.94214113	−309.94230812	−309.94207928
$\lambda = V/T_{el}$	def2-QZVPP	−2.000091	−2.000089	−2.000090
E_{SCF}	ANO	−154.97801428	−154.97798726	−154.97798730
T_{el}	ANO	154.97404078	154.97423120	154.97400504
V	ANO	−309.95205502	−309.95221846	−309.95199230
$\lambda = V/T_{el}$	ANO	−2.000026	−2.000024	−2.000026
E_{SCF}	HUZ-ext	−154.97871729	−154.97868959	−154.97868958
T_{el}	HUZ-ext	154.97746637	154.97766676	154.97743981
V	HUZ-ext	−309.95618366	−309.95655635	−309.95612939
$\lambda = V/T_{el}$	HUZ-ext	−2.000008	−2.000007	−2.000008
E_{CC2}	def2-QZVPP	−155.77507322	−155.77504280	−155.77504049
T_{el}	def2-QZVPP	155.79736761	155.79753924	155.79732864
V	def2-QZVPP	−311.57244083	−311.57258204	−311.57236914
$\lambda = V/T_{el}$	def2-QZVPP	−1.999857	−1.999856	−1.999857

two forms of 2-butyne, but the C–C bond length is slightly larger in its staggered form (for the HF, B3LYP and CCSD(T)-F12 optimized geometries). Has that any importance for the rotational barrier?

The role of the kinetic energy of the electrons

For our own analysis of the reason why the eclipsed form of 2-butyne has a lower energy than its staggered form we proceed in the same way as for our recent analysis of the rotational barrier in ethane.[32] We start from the Schrödinger equation for the motion of the electrons in the fixed nuclear geometries

$$\hat{H}\Psi = (\hat{T}_{el} + \hat{V})\Psi = E\Psi \quad (4)$$

where $\hat{T}_{el}$ is the operator for the kinetic energy of the electrons and $\hat{V}$ contains all the contributions of the potential energy, *i.e.* the Coulomb repulsion of the nuclei and electrons and the nuclear-electronic attraction. We use for our analysis only the quantum mechanical expectation values T_{el} and V of $\hat{T}_{el}$ and $\hat{V}$ calculated with the solution Ψ of the Schrödinger eqn (4) obtained either in the Hartree–Fock or in an approximation including correlation effects (CC2). This means that we base our conclusions exclusively on well-defined quantum mechanical quantities and not on vaguely defined or even artificial decompositions of the total energy. We do not use concepts like steric repulsion where it is not clear how Pauli repulsion, Coulomb repulsion or even other effects are mixed together.

In our analysis of the rotational barrier in ethane[32] we have shown that the decisive quantity is the kinetic energy of the electrons T_{el}. In the staggered form, the electrons of the CH orbitals in one of the two CH_3 groups have the possibility to extend a little into the empty space between the CH orbitals of the other CH_3 group. By this extension the wavefunction of the staggered form will get elongated and slightly smoother, consequently its kinetic energy is getting smaller. But the total energy of the staggered form will also be changed below that of the eclipsed form. Clearly, this is in contradiction to the virial theorem which requires that the total energy and the electronic kinetic energy must have different signs[38,39] at least at geometries which are stationary with respect to the nuclear coordinates. In ethane, it is the change in geometry, in particular the shortening of the C–C distance in the eclipsed form, which will increase T_{el} and correct the ratio between total energy and electronic kinetic energy to $T_{el} = -E$ and will lead to the correct value of the virial quotient, $\lambda = V/T_{el} = -2$.

In order to analyze the situation for 2-butyne, we have again decomposed the total HF energy into the electronic kinetic energy T_{el} and the potential energy V. The results are contained in the Tables 4 and 5. They show that after the rigid rotation (RR) from the eclipsed equilibrium structure to the staggered form, the kinetic energy T_{el} increases by as much as 193.72 × 10^{-6} E_h for the def2-QZVPP basis and similarly for the ANO and HUZ-ext basis sets, 190.42 and 200.39 × 10^{-6} E_h. This is much more than the rather small increase in the HF energy of 26.73, 27.02 and 27.70 × 10^{-6} E_h This strong increase is mainly due to the pair of HOMO orbitals, number 14 and 15, which are essentially the π orbitals of the C≡C bond, building the ring of charge around the C–C≡C–C axis. This is shown in Table 6, which contains the kinetic energies of all occupied orbitals (again except for the C 1s orbitals). The changes in the a-type

Table 5 Changes of the energy components (in 10^{-6} E_h) from the eclipsed to the two staggered forms of 2-butyne, based on HF geometries

Energies	Basis set	ΔE Staggered, RR	ΔE Staggered, FR
E_{SCF}	def2-QZVPP	26.73	26.72
T_{el}	def2-QZVPP	193.72	−35.13
V	def2-QZVPP	−166.99	61.85
E_{SCF}	ANO	27.02	26.98
T_{el}	ANO	190.42	−35.74
V	ANO	−163.44	62.72
E_{SCF}	HUZ-ext	27.70	27.71
T_{el}	HUZ-ext	200.39	−26.56
V	HUZ-ext	−172.69	54.27
E_{CC2}	def2-QZVPP	30.42	32.73
T_{el}	def2-QZVPP	171.63	−38.97
V	def2-QZVPP	−141.21	71.69

This journal is © the Owner Societies 2026

Open Access Article. Published on 22 June 2026. Downloaded on 6/23/2026 3:22:00 AM. This article is licensed under a Creative Commons Attribution 3.0 Unported Licence.

Table 6 Kinetic energies (in E_h) of the orbitals 5 to 15 in the three forms of 2-butyne. HUZ-ext basis set

Orbital Nr.	Irrep	Eclipsed FR	Staggered RR	Staggered FR
5.	a	3.162570	3.162536	3.162527
6.	a	2.665535	2.665515	2.665412
7.	a	3.200506	3.200494	3.200409
8.	a	2.756885	2.756863	2.756818
9.	a	2.816830	2.816820	2.816754
10, 11	e	1.889827	1.889910	1.889934
12, 13	e	1.944837	1.944717	1.944741
14, 15	e	2.281158	2.281353	2.281337

orbitals are rather small, in the order of 50×10^{-6} E_h, the combined effect of the two lower e-type orbitals is of the same size, but the change in the HOMOs is much larger, nearly 200×10^{-6} E_h.

To ascertain that dynamic correlation does not provide an alternative rationale for the trends derived from the HF-based analysis, the data presented in Tables 4 and 5 are complemented by additional calculations at the coupled-cluster level. Unlike the geometry optimisations—where CCSD(T)-F12 calculations could be performed, thereby ensuring that dynamic correlation effects are negligible—the evaluation of the expectation values of the kinetic and potential energies necessarily relies on a less accurate approach. The calculations performed at the CC2 level—an approximation to CCSD— corroborate the findings obtained from the HF calculations and, in particular, reproduce the same qualitative behaviour. These computations were carried out with a local version[40] of the CC2 module[26] implemented in TURBOMOLE.

Fig. 1 presents an explanation for the increased kinetic energy in 2-butyne after the rigid rotation (RR): In acetylene, the electron density of the pair of HOMOs is rotationally symmetric around the C≡C axis. In dimethylacetylene (2-butyne) this rotational symmetry is modified by the interaction with the CH orbitals at the terminal CH_3 groups: In the eclipsed form, the density of the HOMOs 14 and 15, which are essentially the e-type π orbitals of the acetylene-like C≡C bond, is reduced, compared with pure acetylene, by the terminal CH_3 groups at the angles 0°, 120° and 240°, but increased at 60°, 180° and 300°. This results in a pattern with three minima and maxima as shown in Fig. 1a, plotted at a distance (radius) of 1.0 a_0 (a_0: Bohr, the atomic unit of length, 1 a_0 = 0.529177211 Å) from the axis and for $z = 0.0$ a_0, *i.e.* at the center of the C≡C bond, and similarly for all positions z along the C–C≡C–C axis. For the staggered conformer the changes of the density by the terminal CH_3 groups are just opposite for positive and negative values of z and cancel at $z = 0.0$ a_0 (Fig. 1c). The reason is that the π orbitals are more strongly modified by the H atoms close by. That means that the reductions of the density at 0°, 120° and 240° and their increase at 60°, 180° and 300° are caused by the interaction with the hydrogen atoms with positive values of z. And the opposite changes of the density are caused by the interaction with the hydrogen atoms with negative values of z. At $z = 0.0$ a_0 the modification of one CH_3 group cancels the modification of the other one. All this can be seen in Fig. 1b–d. Taking together, this results in six modifications of the total density of the π electrons around the C–C≡C–C axis. The larger number of modifications of the orbitals 14 and 15 in the staggered form of 2-butyne leads to an increase of their kinetic energy. This is evident from Table 6 which shows that their kinetic energies are by about 0.000200 E_h larger in the staggered RR than in the eclipsed FR form, while the changes for the other orbitals are much smaller and have different signs.

Nevertheless, the account has not reached its final stage. In ethane it is the change in the geometry of the eclipsed conformer from its RR to the FR form that leads to the simplified form of the virial theorem, $T_{el} = -E$ and $V = 2 \times E$[38,39] and to a value of −2 for the virial quotient $\lambda = V/T_{el}$.[32,41] Here in 2-butyne, the situation is very similar. Table 1 shows, that in the optimized geometries the C–C distance in the staggered form are slightly larger, by 0.000076 Å in the HF, by 0.000087 Å in the B3LYP and by 0.000072 Å in the CCSD(T)-F12 approximation, than in the eclipsed form, while for both the C≡C and the C–H distances the changes are very small. The C≡C bond is too strong to be changed. By this increase of the C–C distance, the a-type orbitals, in particular the σ-orbitals along the C–C≡C–C chain, are slightly elongated. This is connected with a reduction of their kinetic energies with respect to both the eclipsed FR and the staggered RR forms, as presented in Table 6. The largest change occurs for orbital 7, which is essentially a combination of the two C-C σ bond orbitals. The kinetic energies of the e-type orbitals, on the other hand, which are involved in the π-bonding (or stated differently, which are responsible for the ''hyperconjugation''), remain nearly unchanged. Table 5 summarizes the whole account. The electronic kinetic energy of 2-butyne is increased by about 190×10^{-6} E_h after a rigid rotation (RR) from its eclipsed equilibrium structure to the staggered one, the reoptimization (FR) of the staggered form reduces the kinetic energy again.

Four necessary comments

(1) The two larger basis sets we had used – def2-QZVPP[20] and ANO[28]—were optimized for total energies and resulted in essentially the same HF energy, as contained in Table 2. However, that did not apply for the expectation values of $\hat{T}_{el}$ and $\hat{V}$. Table 4 shows that for the def2-QZVPP basis $-T_{el}$ is quite different from E_{SCF} and the virial quotient λ is quite far from −2. The ANO basis is much better in this respect, but still not perfect. Therefore we have tried a still more flexible basis (HUZ-ext), and Table 4 shows that now E_{SCF} and $-T_{el}$ are nearly identical and λ is close to −2. This is nice, but the main conclusions of our analysis are the same for all the three large basis sets. We can only repeat the comment from Slater's book[39] that whenever one is close to true wavefunction small changes in the energy might be connected with large changes in other properties.

(2) One should be a bit more careful with the expectation values for $\hat{T}_{el}$ and $\hat{V}$. The optimized, fully relaxed (FR) geometries for the eclipsed and staggered forms represent stationary

Open Access Article. Published on 22 June 2026. Downloaded on 6/23/2026 3:22:00 AM.
This article is licensed under a Creative Commons Attribution 3.0 Unported Licence.

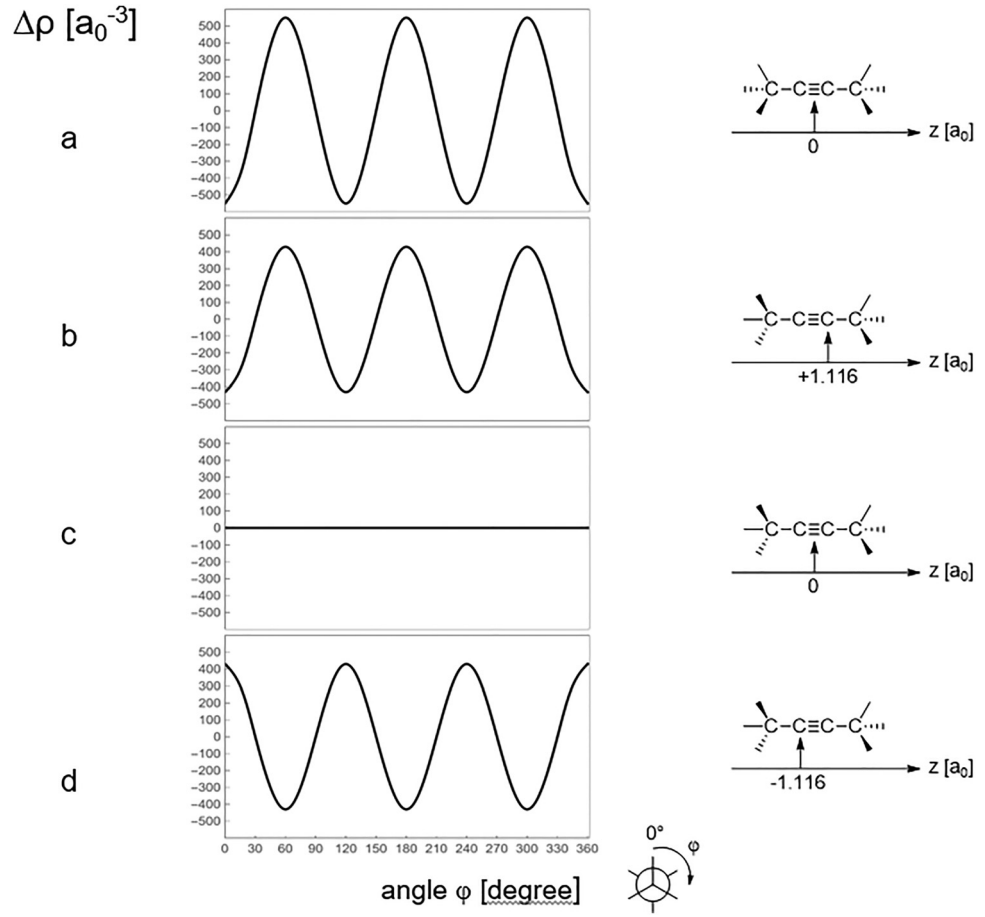

Fig. 1 Change of the density (with respect to the density of acetylene) of the HOMOs 14 and 15, $\Delta\rho$ [a_0^{-3}], as a function of the angle φ, at a distance (radius) of r = 1.0 a_0 from the C–C≡C–C axis. z is the coordinate along the axis, with z = 0.0 a_0 in the center and z = ±1.116 a_0 at the positions of the C atoms.

points on the potential energy surface, therefore the virial theorem is valid in its simplified form: $T_{el} = -E$ and $V = 2 \times E$, or $\lambda = -2$.[38,39] But generally this does not hold true for the RR forms which are no stationary points, therefore the virial forces had to be taken care of.[41] However, for 2-butyne the situation seems to be different. Surprisingly, as Table 4 shows, the value of the virial coefficient λ is also very close to −2 in the staggered RR form, as soon as the large HUZ-ext basis set is used. This means that this form represents also a stationary point. And it is even more surprising that for all basis sets (def2-QZVPP, ANO, HUZ-ext) the same SCF energy is obtained for the staggered RR and the staggered FR structure, while T_{el} and V differ substantially in the two staggered forms.

(3) The two larger basis sets (ANO and HUZ-ext) are slightly linearly dependent: The smallest eigenvalues of the overlap matrix are 0.2D-05 (ANO basis) and 0.7D-08 (HUZ-ext basis). This is taken care of in our SCF code,[23,24] but not in the MCCEPA code.[25] Since the uncertainties in the CEPA energy caused by the linear dependence are in the order of the small rotational barrier itself, Table 2 contains only a CEPA value for the rotation barrier obtained by the def2-QZVPP basis set.

(4) Why the sixfold modification of the rotationally symmetric ring of the electronic density of the π orbitals in acetylene leads to a higher electronic kinetic energy than the threefold modification can be understood by a comparison with the well-known example of the ''particle in a box'' with a potential $V = 0$. In this example, the electronic density of a state with higher energy – and since $V = 0$ this means with higher kinetic energy – has more maxima and minima than that of a state with lower energy. Since the wave functions of the states have to be normalized to unity, $\langle\psi_i|\psi_i\rangle = 1$, the spatial extent of a state with more maxima and minima must be smaller than that of a state with less maxima and minima. Fig. 1 shows that this is indeed the case for the HOMOs of 2-butyne.

Conclusions

The main result of the present study is that the higher stability of the eclipsed conformer of dimethylacetylene, as compared to its staggered conformer, is caused by the kinetic energy of the electrons. The rotationally symmetric ring of the two π orbitals at the central C≡C bond of the C–C≡C–C axis is modified by the C–H bond orbitals at the terminal methyl groups at three angles in the eclipsed form, but at six angles in the staggered form. This leads to a higher electronic kinetic energy and also

This journal is © the Owner Societies 2026

Open Access Article. Published on 22 June 2026. Downloaded on 6/23/2026 3:22:00 AM. This article is licensed under a Creative Commons Attribution 3.0 Unported Licence.

to a higher total molecular energy of the staggered form, as long as the change from the eclipsed to the staggered form is performed by a rigid rotation (RR). But this is in contradiction to the virial theorem which requires that the changes of the total energy and the electronic kinetic energy must have different signs. A reoptimization of the geometry of the staggered conformer to its fully relaxed (FR) form can reestablish the virial theorem, since it leads to a small elongation of the C–C bond distances together with a smoothing of the σ-orbitals of the C–C≡C–C axis and a decrease of the electronic kinetic energy, without a significant change in the total energy.

Conflicts of interest

There are no conflicts to declare.

Data availability

The data supporting this article are either included in the manuscript itself or have been included as part of the supplementary information (SI). Supplementary information is available. See DOI: https://doi.org/10.1039/d5cp04813c.

Acknowledgements

We thank C. Hättig for extending and providing the ricc2 program for the calculation of the expectation values of the kinetic and potential energy. We are also grateful to two anonymous referees for their valuable comments and suggestions.

References

1 B. G. Heising, Action of radon on some unsaturated hydrocarbons, *J. Am. Chem. Soc.*, 1931, **53**, 3245–3263.
2 B. G. Heising and H. M. Davis, Physical constants of dimethylacetylene, *J. Am. Chem. Soc.*, 1935, **57**, 339–340.
3 H. Kaiser, PhD dissertation, Ludwig-Maximilian-University München, 1970.
4 S. Hamai and F. Hirayama, Fluorescence of acetylenic hydrocarbons, *J. Chem. Phys.*, 1979, **71**, 2934–2939.
5 M. H. Palmer and I. C. Walker, The electronic states of but-2-yne studied by VUV absorption, near-threshold electron energy-loss spectroscopy and ab initio configuration interaction methods, *Chem. Phys.*, 2007, **340**, 158–170.
6 U. Jacovella, D. M. P. Holland, S. Boyé-Péronne, B. Gans, N. de Oliveira, D. Joyeux, L. E. Archer, R. R. Lucchese, H. Xu and S. T. Pratt, High-resolution vacuum-ultraviolet photoabsorption spectra of 1-butyne and 2-butyne, *J. Chem. Phys.*, 2015, **143**, 034304.
7 U. Jacovella, D. M. P. Holland, S. Boyé-Péronne, B. Gans, N. de Oliveira, K. Ito, D. Joyeux, L. E. Archer, R. R. Lucchese, H. Xu and S. T. Pratt, A Near-Threshold Shape Resonance in the Valenc-Shell Photoabsorption of Linear Alkynes, *J. Phys. Chem. A*, 2015, **119**, 12339–12348.
8 H. Xu, U. Jacovella, B. Ruscic, S. T. Pratt and R. R. Lucchese, Near-threshold shape resonance in the photoionization of 2-butyne, *J. Chem. Phys.*, 2012, **136**, 154303.
9 C. Jungen and S. T. Pratt, An energy-modified quantum defect method for the analysis of Rydberg spectra: Application to 2-butyne, *J. Chem. Phys.*, 2024, **161**, 094107.
10 P. R. Bunker, J. W. C. Johns, A. R. W. McKellar and C. di Lauro, Dimethylacetylene: Internal Rotation and the Analysis of the Methyl Rocking Torsion Infrared Fundamental Band, *J. Mol. Spectr.*, 1993, **162**, 142–151.
11 C. di Lauro, P. R. Bunker, J. W. C. Johns and A. R. W. McKellar, The Rotation-Torsion Structure in the $\nu 11/\nu 15$ **(Gs)** Methyl Rocking Fundamental Band of Dimethylacetylene, *J. Mol. Spectr.*, 1997, **184**, 177–185.
12 O. Omorodion, M. Bober and K. J. Donald, Turn: Weak Interactions and Rotational Barriers in Molecules – Insights from Substituted Butynes, *J. Phys. Chem. A*, 2016, **120**, 8896–8906.
13 G. P. Moss, Basic Terminology of Stereochemistry, *Pure Appl. Chem.*, 1996, **68**, 2193–2222.
14 K. N. Houk, L. T. Scott, N. G. Rondan, D. C. Spellmeyer, G. Reinhardt, J. L. Hyun, G. J. DeCicco, R. Weiss, M. H. M. Chen, L. S. Bass, J. Clardy, F. S. Jørgensen, T. A. Eaton, V. Sarkozi, C. M. Petit, L. Ng and K. D. Jordan, Pericyclynes: ''Exploded Cycloalkanes'' with Unusual Orbital Interactions and Conformational Properties. MM2 and STO-3G Calculations, X-ray Crystal Structures, Photoelectron Spectra, and Electron Transmission Spectra, *J. Am. Chem. Soc.*, 1985, **107**, 6556–6562.
15 V. Maraval and R. Chauvin, From Macrocyclic Oligoacetylenes to Aromatic Ring Carbo-mers, *Chem. Rev.*, 2006, **106**, 5317–5343.
16 S. Toyota, Rotational Isomerism Involving Acetylene Carbon, *Chem. Rev.*, 2010, **110**, 5398–5424.
17 M. G. Miksic, E. Segerman and B. Post, The Solid Phase Transformation in Dimethylacetylene at −119 °C, *Acta Cryst.*, 1959, **12**, 390–393.
18 M. Tanimoto, K. Kuchitsu and Y. Morino, Bond Lengths of Dimethylacetylene as Determined by Gas Electron Diffraction, *Bull. Chem. Soc.*, 1969, **42**, 2519–2523.
19 TURBOMOLE, a development of University of Karlsruhe and Forschungszentrum Karlsruhe GmbH, 1989-2007, TURBOMOLE GmbH, since 2007, available from https://www.turbomole.com.
20 F. Weigend, F. Furche and R. Ahlrichs, Gaussian basis sets of quadruple zeta valence quality for atoms H-Kr, *J. Chem. Phys.*, 2003, **119**, 12753–12762.
21 C. Hättig, D. P. Tew and A. Köhn, Accurate and efficient approximations to explicitly correlated coupled-cluster singles and doubles, CCSD-F12, *J. Chem. Phys.*, 2010, **132**, 231102/1–231102/4.
22 F. Weigend and R. Ahlrichs, Balanced basis sets of split valence, triple zeta valence and quadruple zeta valence quality for H to Rn: Design and assessment of accuracy, *Phys. Chem. Chem. Phys.*, 2005, **7**, 3297–3305.
23 V. Staemmler, Note on Open Shell Restricted SCF Calculations for Rotation Barriers about C-C Double Bonds: Ethylene and Allene, *Theoret. Chim. Acta*, 1977, **45**, 89–94.

Open Access Article. Published on 22 June 2026. Downloaded on 6/23/2026 3:22:00 AM.
This article is licensed under a Creative Commons Attribution 3.0 Unported Licence.

24 All the parts necessary for the present analysis were added later into the original code of ref. 23.
25 R. Fink and V. Staemmler, A multi-configuration reference CEPA method based on pair natural orbitals, *Theoret. Chim. Acta*, 1993, **87**, 129–145.
26 C. Hättig and F. Weigend, CC2 excitation energy calculations on large molecules using the resolution of the identity approximation, *J. Chem. Phys.*, 2000, **113**, 5154–5161.
27 A. K. Wilson, T. van Mourik and T. H. Dunning, *J. Mol. Struct. (THEOCHEM)*, 1996, **388**, 339–349.
28 P.-O. Widmark, P.-Å. Malmqvist and B. O. Roos, Density matrix averaged atomic natural orbital (ANO) basis sets for correlated molecular wave functions. I. First row atoms, *Theor. Chim. Acta*, 1990, **77**, 291–306.
29 (*a*) S. Huzinaga, Gaussian-Type Functions for Polyatomic Systems, *I. J. Chem. Phys.*, 1965, **42**, 1293–1302; (*b*) S. Huzinaga and M. Klobukowski, Well-tempered Gaussian basis set expansions of Roothaan-Hartree-Fock atomic wavefunctions for lithium through mercury, *J. Mol. Struct. THEOCHEM*, 1988, **167**, 1–210.
30 F. M. Bickelhaupt and E. J. Baerends, The Case for Steric Repulsion Causing the Staggered Conformation of Ethane, *Angew. Chem., Int. Ed.*, 2003, **42**, 4183–4186.
31 V. Pophristic and L. Goodman, Hyperconjugation not steric repulsion leads to the staggered structure of ethane, *Nature*, 2001, **411**, 565–568.
32 V. Staemmler and R. Franke, On the Origin of the Rotational Barrier in Ethane, *J. Comput. Chem.*, 2025, **46**, e70014, DOI: 10.1002/jcc.70014.
33 W. Kutzelnigg, Einführung in die Theoretische Chemie. *Band 2: Die chemische Bindung*, Verlag Chemie, Weinheim, New York, 1978, pp. 92–104.
34 I. N. Levine, *Quantum Chemistry*, Prentice-Hall International, Englewood Cliffs, New Jersey, 4th edn, 1991, pp. 549–572.
35 R. S. Mulliken, C. A. Rieke and W. C. Brown, Hyperconjugation, *J. Am. Chem. Soc.*, 1941, **63**, 41–56.
36 R. S. Mulliken and C. A. Rieke, Improved computations on conjugation and hyperconjugation, *J. Am. Chem. Soc.*, 1941, **63**, 1770–1771.
37 F. Jensen, *Introduction to Computational Chemistry*, John Wiley & Sons, Chichester, 1999, pp. 63–64.
38 J. C. Slater, The Virial and Molecular Structure, *J. Chem. Phys.*, 1933, **1**, 687–691.
39 J. C. Slater, *Quantum Theory of Molecules and Solids, Volume 1. Electronic Structure of Molecules*, McGraw-Hill, New York, 1963, pp. 29–34, pp. 57–59.
40 C. Hättig, 2026, private communication.
41 R. F. W. Bader, J. R. Cheeseman, K. E. Laidig, K. W. Wiberg and C. Breneman, Origin of Rotation and Inversion Barriers, *J. Am. Chem. Soc.*, 1990, **112**, 6530–6536.

 This journal is © the Owner Societies 2026